International Journal of Recent Technology and Engineering (IJRTE)
ISSN: 2277-3878 (Online), Volume-9 Issue-5, January 2021

Modelling, Simulation and Control of Robotic Hand using Virtual Prototyping Technology

Ranashree Das, Dhrubajyoti Gupta

Abstract*: Hand is one of the most important body parts of a human being that exhibits extremely complex motional behaviors. So, accurate design of a prosthetic hand with precise motion has been a very challenging job for researchers over a few decades. Moreover, selection of materials, actuators, sensors, etc. becomes tedious which prior knowledge of the probable outcomes of a particular design. This paper presents an organized procedure to design and solve the kinematics, dynamics and trajectory control problem of a robotic hand. Denavit- Hartenberg method was used for the kinematic analyses and Lagrange-Euler formulation applied on basic rotational mechanics was used for the dynamic analyses of the robotic hand. To reduce difficulty, three degrees of freedom has been assigned to each finger. MATLAB codes were written to develop the mathematical model and carry out the theoretical calculations. The results so obtained were verified with the actual simulation results of the design which were obtained from ADAMS and hence validating the design. Finally, a PID controller was implemented using ADAMS-MATLAB CO-SIMULATATION technique, for controlling the hand, so as to achieve the desired motion. By the virtue of the results obtained the choice of materials, actuators, sensors, etc. becomes easier in case of the physical prototype which is the primal essence of virtual prototyping.

***Index Terms*: Kinematics, Dynamics, Virtual Prototyping technology, PID Controller, Co- Simulation.**

I. INTRODUCTION

In the field of robotics, hand design has been one of the most interesting topics for researchers over a past few years for its versatile applications such as shortening the metal component [1], fruit picking [2], drawing, welding, bomb defusing [3] etc. Its diversity is extended further in the form of exoskeletons that provides the base of rehabilitation robotics [4]. These robots are designed according to the function and shape of the human body and the user will be able to control the robotic limbs. These robotic limbs may be active or passive depending on the user application. But still the exact movement of the human hand is still unsolved because of its complicated structure. So, without knowledge of its basic anatomy, the design of the hand model is quite challenging. The structure of the hand includes bones and joints, ligaments and tendons, muscles, nerves, circulatory system, and skin; however, this paper only focused in area of bones and joints.

Manuscript received on August 24, 2020.
Revised Manuscript received on January 28, 2021.
Manuscript published on January 30, 2021.
Ranashree Das, Research scholar, Mechanical engineering department, NIT Durgapur, Durgapur, west Bengal, India.
Dhrubajyoti Gupta, UG student, Mechanical engineering department, NIT Durgapur, Durgapur, west Bengal, India.

The basic parts of the human hand are; wrist, palm and five fingers (thumb, index finger, middle finger, ring finger, and little finger) [5], that are shown in Fig 1. Actually, the human hand has total twenty-seven bones including wrist bones [6]. The arrangement of these bones is different at different positions of hand viz. eight carpal bones are arranged in a wrist but in two set of rows, each set carries four bones, palms have total five long metacarpal bones that connects every finger individually and the remaining fourteen phalangeal bones are positioned at four fingers and the thumb [5]. The details about bones and joints of human hand has been shown in Fig 1 [7]. Joints not only make a bridge among the different bones but also give the motion to the fingers. There are five types of joints present in the hand, from wrist to the end of the fingers which are CMC, MCP, IP, PIP and DIP that has shown in Fig 1 [7]. CMC joint connects carpal bones and metacarpal bones and MCP joint connects metacarpal bones and phalanges of every finger. There are some differences among DIP, PIP and IP joints. The IP joint is present only in thumb in between its proximal and distal phalangeal whereas PIP and DIP joints connect the proximal with the middle phalangeal and the middle with the distal phalangeal respectively of the rest of the fingers [5], [8].

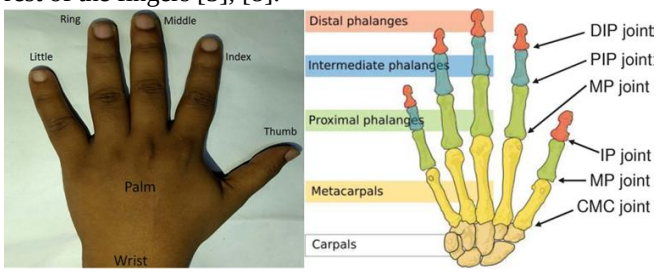

Fig 1: The human hand and the bones and joints human hand [7].

Based on the joints and bones, the human hand motion is divided into two categories the flexion/extension and abduction / adduction. Flexion/extension means rotation of finger towards and away from the palm but it occurs in a plane perpendicular to the palm and abduction / adduction means spreading and closing of the fingers occurring in a plane parallel to the palm [9]. Depending on the type of motion different angular displacements are fixed for every joint in the finger. In order to achieve all these ranges of motion and make the robotic hand more accurate, different researchers assign different degrees of freedom to their model. Degrees of freedom decide the minimum number of independent parameters required to describe a system exactly [10]. Higher degrees of freedom complexifies the design extremely. So, careful choice of degrees of freedom stands important for a simple and yet elegant manipulator design.

The design of a simple manipulator in real life by considering all the above standards requires fixation of a lot of parameters like mechanism, material, actuator, sensors etc. Development of the device by trial-and-error method is very much time consuming as well as uneconomical.

To overcome this inadequacy, this paper gives an idea about virtual prototyping (VP) technology that is quite cost effective and time saving also. Virtual prototyping (VP) technology means execution of the motion algorithms on a virtual model and refining its performance prior to development of a physical prototype [11]. In this paper the kinematics, dynamics and control problem of the hand has been solved based on VP technology. This paper mainly focuses on three distinguish areas namely kinematics, dynamics and control. The kinematics has got two parts a) Forward kinematics, b) Inverse kinematics. Forward kinematics deals with the determination of the position of the end effector from the given joint angle motion [10]. The position obtained from the forward kinematics has been mapped to the global coordinate system of ADAMS software which is one of another difficult issue for every simulation-based analysis [5]. In inverse kinematics, the joint angles are calculated from given position and orientation of end effector by using simple algebraic method. The velocity and acceleration analysis has also been carried out for the joints as well as the end effectors. The dynamic analysis of the hand is sub- dived into 3 parts a) motion dynamic analysis without considering the static force b) static force analysis and c) motion dynamic analysis along with the static force [12]. In motion dynamic analysis without considering the static force, the dynamic equations have been solved by following the Lagrange-Euler method. Most of the papers follow generalized dynamic equation to solve dynamics problems [5], on the other hand this article goes through the basic rotational mechanics in order to carry out the dynamic analyses [5]. This method is more powerful in order to get a clear insight of the matter. In static force analysis, a simple relationship has been made between the joint torque vector for each joint (τ_{si}) and end effector load (F) vector [12]. A continuous static force analysis curve has been plotted in MATLAB which is another important aspect of this paper. Since all the joints need to be fixed at every position, continuous curve of static force could not be obtained in ADAMS. Finally, the complete dynamic solution is obtained by combining both motion dynamics and static force analysis. After that, a simple PID controller was developed using the ADAMS-MATLAB co-simulation strategy which is another powerful aspect of this analysis [13], [14], [15].

II. DESIGN OF THE HAND

It is needless to mention that the design is inspired from human hand with little alterations to the degrees of freedom. The thumb has got three degrees of freedom with joint axis of the first joint being perpendicular to the other two. The rest of the fingers also have three degrees of freedom but all the joint axes are parallel in this case. CATIA was used for the design purpose. The design is shown below Figure: 2.1

Fig 2: Catia model

This design was used for the detailed analyses the steps of which are listed below:

i. The hand was designed as stated above.

ii. MATLAB codes were written to carry out the theoretical analysis.

iii. The design was imported in MSC ADAMS.

iv. Simulation of the model was carried out in ADAMS by giving joint motions.

v. The results of simulation (ADAMS) and the theoretical calculations (MATLAB) were compared so as to validate the experiment.

Fig 3: Hand model imported to ADAMS: (a) Before simulation (b) After simulation

The detailed theoretical analyses have been carried in the followed sections.

III. KINEMATICS ANALYSIS OF THE HAND

Robot kinematics deals with the study of motion of the robot without taking into account the cause of motion. In this section the kinematic analysis of each finger has been carried out in detail. Robot kinematics has got two phases viz. (1) Forward Kinematics and (2) Inverse Kinematics. The former deals with determining the position and orientation of end effector with the known joint variables whereas the later deals with determination of the joint variables while the position and orientation of the end effector is known [5]. However, the analysis in this section does not merely hover around position analysis only. The velocity and acceleration analysis of the joints and the end effector has also been carried out in the subsequent sections.

A. Kinematics of thumb

The DH Parameter of the thumb is shown below:

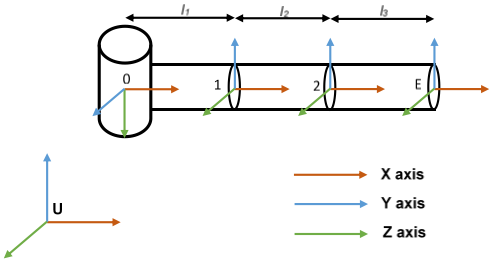

Fig 4: Denavit- Hartenberg parameter model of thumb

Table 1: Denavit- Hartenbag parameter of Thumb

Frame	θ_i (degree)	d_i (mm)	α_i (degree)	a_i (mm)
0-1	θ_1	0	-90	l_1= 32
1-2	θ_2	0	0	l_2= 39
2-E	θ_3	0	0	l_3= 47

Forward Kinematics of thumb

Each joint has been assigned a cubic trajectory: $\theta_i = a_0 + a_1 t + a_2 t^2 + a_3 t^3$ .The range of motions of each joint has been presented below:

Table 2: Range of motion of each joint of thumb

θ_i	θ_i (deg)	θ_f (deg)	$\dot{\theta}_i$ (deg/s)	$\dot{\theta}_f$ (deg/s)	t_i (s)	t_f (s)
$\theta_1 = 540t^2 - 360t^3$	0	180	0	0	0	1
$\theta_2 = 72t^2 - 48t^3$	0	24	0	0	0	1
$\theta_3 = 72t^2 - 48t^3$	0	24	0	0	0	1

The position and orientation of a frame with respect to its previous frame is given by the following homogeneous transformation matrix:

$$ {}^{i-1}_{i}T = \begin{bmatrix} C\theta_i & -S\theta_i C\alpha_i & S\theta_i S\alpha_i & a_i C\theta_i \\ S\theta_i & C\theta_i C\alpha_i & -C\theta_i S\alpha_i & a_i S\theta_i \\ 0 & S\alpha_i & C\alpha_i & d_i \\ 0 & 0 & 0 & 1 \end{bmatrix} $$

Where $C\theta_i = \cos\theta_i$, $S\theta_i = \sin\theta_i$, $C\alpha_i = \cos\alpha_i$ $S\alpha_i = \sin\alpha_i$

$$ {}^{0}_{E}T = {}^{0}_{1}T \times {}^{1}_{2}T \times {}^{2}_{E}T \qquad (1) $$

Equation (1) represents the homogenous transformation matrix of end effector frame with respect to the base coordinate frame.

$$ {}^{0}_{E}T = \begin{bmatrix} C\theta_1 C(\theta_2+\theta_3) & -C\theta_1 S(\theta_2+\theta_3) & -S\theta_1 & l_1 C\theta_1 + l_2 C\theta_1 C\theta_2 + l_3 C\theta_1 C(\theta_2+\theta_3) \\ S\theta_1 C(\theta_2+\theta_3) & -S\theta_1 S(\theta_2+\theta_3) & C\theta_1 & l_1 S\theta_1 + l_2 S\theta_1 C\theta_2 + l_3 S\theta_1 C(\theta_2+\theta_3) \\ -S(\theta_2+\theta_3) & -C(\theta_2+\theta_3) & 0 & -l_2 S\theta_2 - l_3 S(\theta_2+\theta_3) \\ 0 & 0 & 0 & 1 \end{bmatrix} $$

Where, $\theta_{23} = \theta_2 + \theta_3$ and $\theta_{123} = \theta_1 + \theta_2 + \theta_3$

However, the universal reference frame is not same as that of the first joint frame. So, a series of transformations has been carried out in order to get the position and orientation with respect to the universal reference frame. The transformations are shown below:

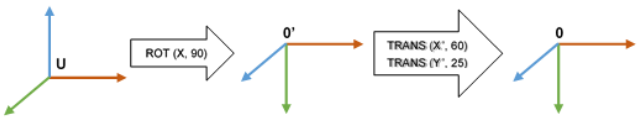

Fig 5: Position mapping model of thumb

The mapping matrix is given by:

$$ H = Rot(X, 90^0) \times Trans(X', 60) \times Trans(Y', 25) \quad (2) $$

$$ H = \begin{bmatrix} 1 & 0 & 0 & 0 \\ 0 & C90^0 & -S90^0 & 0 \\ 0 & S90^0 & C90^0 & 0 \\ 0 & 0 & 0 & 1 \end{bmatrix} \times \begin{bmatrix} 1 & 0 & 0 & 60 \\ 0 & 1 & 0 & 25 \\ 0 & 0 & 1 & 0 \\ 0 & 0 & 0 & 1 \end{bmatrix} $$

$$ H = \begin{bmatrix} 1 & 0 & 0 & 0 \\ 0 & 0 & -1 & 0 \\ 0 & 1 & 0 & 0 \\ 0 & 0 & 0 & 1 \end{bmatrix} \times \begin{bmatrix} 1 & 0 & 0 & 60 \\ 0 & 1 & 0 & 25 \\ 0 & 0 & 1 & 0 \\ 0 & 0 & 0 & 1 \end{bmatrix} $$

$$ H = \begin{bmatrix} 1 & 0 & 0 & 60 \\ 0 & 0 & -1 & 0 \\ 0 & 1 & 0 & 25 \\ 0 & 0 & 0 & 1 \end{bmatrix} $$

The final position and orientation matrix with respect to the universal frame is given by:

$$ {}^{U}_{E}T = H \times {}^{0}_{E}T \qquad (3) $$

$$ {}^{U}_{E}T = \begin{bmatrix} C\theta_1 C\theta_{23} & -C\theta_1 S\theta_{23} & -S\theta_1 & l_1 C\theta_1 + l_2 C\theta_1 C\theta_2 + l_3 C\theta_1 C\theta_2 C\theta_3 - l_3 C\theta_1 S\theta_2 S\theta_3 + 60 \\ S\theta_{23} & C\theta_{23} & 0 & l_2 S\theta_2 + l_3 S\theta_{23} \\ S\theta_1 C\theta_{23} & -S\theta_1 S\theta_{23} & C\theta_1 & l_1 S\theta_1 + l_2 S\theta_1 C\theta_2 + l_3 S\theta_1 C\theta_2 C\theta_3 - l_3 S\theta_1 S\theta_2 S\theta_3 + 25 \\ 0 & 0 & 0 & 1 \end{bmatrix} $$

So, the position of the end effector is given as:

$$ X = l_1 C\theta_1 + l_2 C\theta_1 C\theta_2 + l_3 C\theta_1 C\theta_2 C\theta_3 - l_3 C\theta_1 S\theta_2 S\theta_3 + 60 \quad (4) $$

$$ Y = l_2 S\theta_2 + l_3 S\theta_{23} \quad (5) $$

$$ Z = l_1 S\theta_1 + l_2 S\theta_1 C\theta_2 + l_3 S\theta_1 C\theta_2 C\theta_3 - l_3 S\theta_1 S\theta_2 S\theta_3 + 25 \quad (6) $$

Inverse kinematics of thumb

In this section, joint variables are determined with the known position and orientation matrix of the end effector. However, in this case, the matrix will be with respect to the first joint frame rather than the universal frame ($ {}^{0}_{E}T $).

Let assume,

$$\begin{bmatrix} C\theta_1C(\theta_2+\theta_3) & -C\theta_1S(\theta_2+\theta_3) & -S\theta_1 & l_1C\theta_1+l_2C\theta_1C\theta_2+l_3C\theta_1C(\theta_2+\theta_3) \\ S\theta_1C(\theta_2+\theta_3) & -S\theta_1S(\theta_2+\theta_3) & C\theta_1 & l_1S\theta_1+l_2S\theta_1C\theta_2+l_3S\theta_1C(\theta_2+\theta_3) \\ -S(\theta_2+\theta_3) & -C(\theta_2+\theta_3) & 0 & -l_2S\theta_2-l_3S(\theta_2+\theta_3) \\ 0 & 0 & 0 & 1 \end{bmatrix} = \begin{bmatrix} r_{11} & r_{12} & r_{13} & p_x \\ r_{21} & r_{22} & r_{23} & p_y \\ r_{31} & r_{32} & r_{33} & p_z \\ 0 & 0 & 0 & 1 \end{bmatrix}$$

Multiplying both sides by ${}^{0}_{1}T^{-1}$

$$\begin{bmatrix} C\theta_{23} & -S\theta_{23} & 0 & l_2C\theta_2+l_3C\theta_{23} \\ S\theta_{23} & C\theta_{23} & 0 & l_2S\theta_2+l_3S\theta_{23} \\ 0 & 0 & 1 & 0 \\ 0 & 0 & 0 & 1 \end{bmatrix} = \begin{bmatrix} r_{11}C\theta_1+r_{21}S\theta_1 & r_{12}C\theta_1+r_{22}S\theta_1 & r_{13}C\theta_1+r_{23}S\theta_1 & p_xC\theta_1+p_yS\theta_1-l_1 \\ -r_{31} & -r_{32} & -r_{33} & -p_z \\ -r_{11}S\theta_1+r_{21}C\theta_1 & -r_{12}S\theta_1+r_{22}C\theta_1 & -r_{13}S\theta_1+r_{23}C\theta_1 & -p_xS\theta_1+p_yC\theta_1 \\ 0 & 0 & 0 & 1 \end{bmatrix}$$

Comparing both sides and solving the equations, the angles are given by:

$$\theta_1 = \tan^{-1}\frac{p_y}{p_x} \qquad (7)$$

$$\theta_2 = \sin^{-1}\frac{l_3r_{31}-p_z}{l_2} \qquad (8)$$

$$\theta_3 = \tan^{-1}\frac{r_{31}}{r_{32}} - \theta_2 \qquad (9)$$

Velocity and acceleration analysis of thumb

The joint trajectories have already been defined as:

$$\theta_1 = 540t^2 - 360t^3$$

$$\theta_2 = 72t^2 - 48t^3$$

$$\theta_3 = 72t^2 - 48t^3$$

Therefore, the joint velocities are:

$$\dot{\theta}_1 = \frac{d\theta_1}{dt}, \dot{\theta}_2 = \frac{d\theta_2}{dt}, \dot{\theta}_3 = \frac{d\theta_3}{dt} \qquad (10)$$

The joint accelerations are:

$$\ddot{\theta}_1 = \frac{d\dot{\theta}_1}{dt}, \ddot{\theta}_2 = \frac{d\dot{\theta}_2}{dt}, \ddot{\theta}_3 = \frac{d\dot{\theta}_3}{dt} \qquad (11)$$

From the forward kinematics, the position of the end effector as:

$$X = l_1C\theta_1 + l_2C\theta_1C\theta_2 + l_3C\theta_1C\theta_2C\theta_3 - l_3C\theta_1S\theta_2S\theta_3 + 60$$

$$Y = l_2S\theta_2 + l_3S\theta_{23}$$

$$Z = l_1S\theta_1 + l_2S\theta_1C\theta_2 + l_3S\theta_1C\theta_2C\theta_3 - l_3S\theta_1S\theta_2S\theta_3 + 25$$

The velocity of the end effector is given by:

$$\dot{X} = \frac{dX}{dt}, \dot{Y} = \frac{dY}{dt}, \dot{Z} = \frac{dZ}{dt} \qquad (12)$$

The acceleration of the end effector is given by:

$$\ddot{X} = \frac{d\dot{X}}{dt}, \ddot{Y} = \frac{d\dot{Y}}{dt}, \ddot{Z} = \frac{d\dot{Z}}{dt} \qquad (13)$$

B. Kinematics of rest fingers

Rest of the fingers are identical with link lengths being the only variant. So, their analysis remains same, parametrically. The DH parameter representation of the fingers is shown below (just for reference the numerical values of the index fingers are shown):

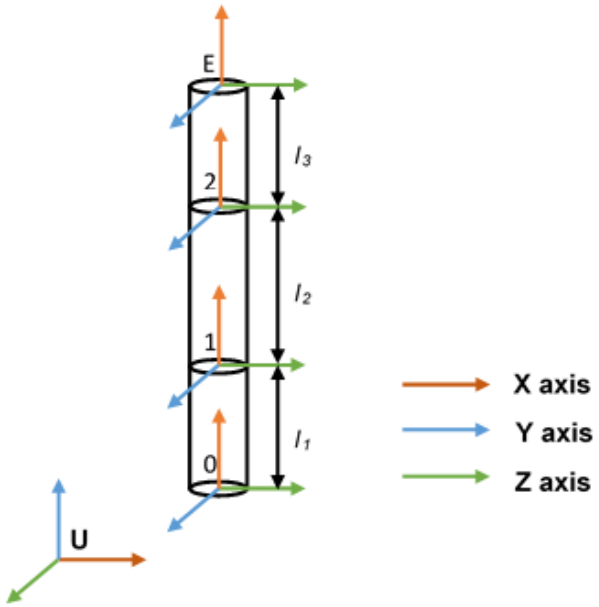

Fig 6: Denavit- Hartenberg parameter model of Index finger

Table 3: Denavit- Hartenbag parameter of index finger

Frame	$\theta_{i(\text{degree})}$	$d_{i(\text{mm})}$	$\alpha_{i(\text{degree})}$	$a_{i(\text{mm})}$
0-1	θ_1	0	0	l_1= 31
1-2	θ_2	0	0	l_2= 27
2-E	θ_3	0	0	l_3= 29

Forward Kinematics of rest finger

Once again, cubic trajectory has been assigned to each joint: $\theta_i = a_0 + a_1t + a_2t^2 + a_3t^3$ .The range of motions of each joint has been presented below in Table 4:

Table 4: Range of motion of each joint of index finger

θ_i	θ_i (deg)	θ_f (deg)	$\dot{\theta}_i$ (deg/s)	$\dot{\theta}_f$ (deg/s)	t_i (s)	t_f (s)
$\theta_1 = 135t^2 - 90t^3$	0	180	0	0	0	1

$\theta_2 = 120t^2 - 80t^3$	0	24	0	0	0	1
$\theta_3 = 120t^2 - 80t^3$	0	24	0	0	0	1

The position and orientation of a frame with respect to its previous frame is given by the following homogeneous transformation matrix:

$$ {}^{i-1}_{i}T = \begin{bmatrix} C\theta_i & -S\theta_2 C\alpha_i & S\theta_i S\alpha_i & a_i C\theta_i \\ S\theta_i & C\theta_i C\alpha_i & -C\theta_i S\alpha_i & a_i S\theta_i \\ 0 & S\alpha_i & C\alpha_i & d_i \\ 0 & 0 & 0 & 1 \end{bmatrix} $$

Where, $C\theta_i = \cos\theta_i$, $S\theta_i = \sin\theta_i$,

$C\alpha_i = \cos\alpha_i$ $S\alpha_i = \sin\alpha_i$

$$ {}^{0}_{E}T = {}^{0}_{1}T \times {}^{1}_{2}T \times {}^{2}_{E}T $$

Similar from Equation (1) represents the homogenous transformation matrix of end effector frame with respect to the base coordinate frame.

$$ {}^{0}_{E}T = \begin{bmatrix} C\theta_{123} & -S\theta_{123} & 0 & L_1C\theta_1 + L_2C\theta_{12} + L_3C\theta_{123} \\ S\theta_{123} & -C\theta_{123} & 0 & L_1S\theta_1 + L_2S\theta_{12} + L_3S\theta_{123} \\ 0 & 0 & 1 & 0 \\ 0 & 0 & 0 & 1 \end{bmatrix} $$

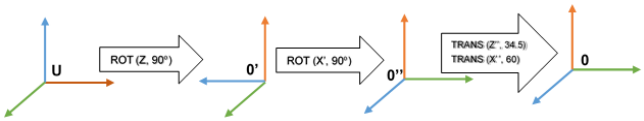

Fig 7: Position mapping model of thumb

The mapping is given by: $H = Rot(Z,90^0) \times Rot(X',90^0) \times Trans(Z'',34.5) \times Trans(X'',60)$ (14)

$$ H = \begin{bmatrix} C90^0 & -S90^0 & 0 & 0 \\ S90^0 & C90^0 & 0 & 0 \\ 0 & 0 & 1 & 0 \\ 0 & 0 & 0 & 1 \end{bmatrix} \times \begin{bmatrix} 1 & 0 & 0 & 0 \\ 0 & C90^0 & -S90^0 & 0 \\ 0 & S90^0 & C90^0 & 0 \\ 0 & 0 & 0 & 1 \end{bmatrix} \times \begin{bmatrix} 1 & 0 & 0 & 60 \\ 0 & 1 & 0 & 0 \\ 0 & 0 & 1 & 34.5 \\ 0 & 0 & 0 & 1 \end{bmatrix} $$

$$ H = \begin{bmatrix} 0 & -1 & 0 & 0 \\ 1 & 0 & 0 & 0 \\ 0 & 0 & 1 & 0 \\ 0 & 0 & 0 & 1 \end{bmatrix} \times \begin{bmatrix} 1 & 0 & 0 & 0 \\ 0 & 0 & -1 & 0 \\ 0 & 1 & 0 & 0 \\ 0 & 0 & 0 & 1 \end{bmatrix} \times \begin{bmatrix} 1 & 0 & 0 & 60 \\ 0 & 1 & 0 & 0 \\ 0 & 0 & 1 & 34.5 \\ 0 & 0 & 0 & 1 \end{bmatrix} $$

$$ H = \begin{bmatrix} 0 & 0 & 1 & 34.5 \\ 1 & 0 & 0 & 60 \\ 0 & 1 & 0 & 0 \\ 0 & 0 & 0 & 1 \end{bmatrix} $$

The final position and orientation matrix with respect to the universal frame is given by similar equation (3):

$$ {}^{U}_{E}T = H \times {}^{0}_{E}T $$

$$ {}^{U}_{E}T = \begin{bmatrix} 0 & 0 & 1 & 34.5 \\ C\theta_{123} & -S\theta_{123} & 0 & l_1C\theta_1 + l_2C\theta_{12} + l_3C\theta_{123} + 60 \\ S\theta_{123} & C\theta_{123} & 0 & l_1S\theta_1 + l_2S\theta_{12} + l_3S\theta_{123} \\ 0 & 0 & 0 & 1 \end{bmatrix} $$

So, the position of the end effector is given as:

$$ X = 34.5 \qquad (15) $$

$$ Y = l_1C\theta_1 + l_2C\theta_{12} + l_3C\theta_{123} + 60 \qquad (16) $$

$$ Z = l_1S\theta_1 + l_2S\theta_{12} + l_3S\theta_{123} \qquad (17) $$

Inverse Kinematics of rest finger

It turns out that the inverse kinematic solutions of the other three fingers is same as that of a standard 3 link planar arm. Therefore, the solutions are

$$ \theta_2 = \cos^{-1}\frac{w_x^{\,2} + w_y^{\,2} - l_1^{\,2} - l_2^{\,2}}{2l_1l_2} \qquad (18) $$

$$ \theta_1 = \sin^{-1}\frac{(l_1 + l_2\cos\theta_2)w_y - l_2\sin\theta_2 w_x}{\Delta} \qquad (19) $$

$$ \theta_3 = \cos^{-1}\frac{X - l_1\cos\theta_1 - l_2\cos(\theta_1 + \theta_2)}{l_3} - \theta_1 - \theta_2 \qquad (20) $$

Where

$w_x = X$ coordinate of 2nd joint

$w_y = Y$ coordinate of 2nd joint

$$ \Delta = l_1^{\,2} + l_2^{\,2} + 2l_1l_2\cos\theta_2 = w_x^{\,2} + w_y^{\,2} $$

Velocity and acceleration analysis of rest finger

The velocity and acceleration analysis is similar to that of the thumb.

IV. DYNAMIC ANALYSIS OF THE HAND

Dynamic analysis is one of the major parts of robotic manipulation and development of control algorithm. Dynamic analysis basically deals with the calculation of joint forces or torques, when a body is in a state of motion or rest. Force calculation for body in rest is called static force analysis and when it is applied on a moving body is called kinetics. However, the sense of practicality lies on the combination of both the cases. The Lagrange- Euler formulation has been used for calculation of joint torques.

This method utilizes the kinetic energy and potential energy of the hand manipulator. The deformability of the body was completely ignored here. In this section, the dynamic analysis of the hand manipulator has been carried out in three different ways A) motion dynamics without static force B) static force analysis and C) motion dynamics with static force. All the analyses have been done for thumb and index finger. The analyses of the other three fingers are similar to that of the index fingers. The detailed methodology of the dynamic analyses is as follows.

A. Motion dynamics without static force

The basic idea behind this is to find out the joint torques when a serial manipulator is moving from one place to another one without considering the end effector force. The equation of the joint torque is

$$\tau_i = \frac{d}{dt}\left(\frac{\delta L}{\delta \dot{\theta}_i}\right) - \frac{\delta L}{\delta \theta_i} \qquad (21)$$

Where, τ_i = torque on ith joint

L= Lagrangian

L can be defined as given below

L= K-P

K = kinetic energy

P= potential energy

θ_i = angular displacement of ith rotational joint

$\dot{\theta}_i$ = angular velocity of ith rotational joint

Torque calculation for thumb

In this design, the thumb has three degrees of freedom. The second and the third joint moves in a plane perpendicular to the plane of motion of the first joint. Clearly, there are three joint torques. The full analyses are given below:

Development of Joint torque equation for thumb

Before finding out the equations of the joint torques, it is necessary to compute kinetic and potential energy of every link.

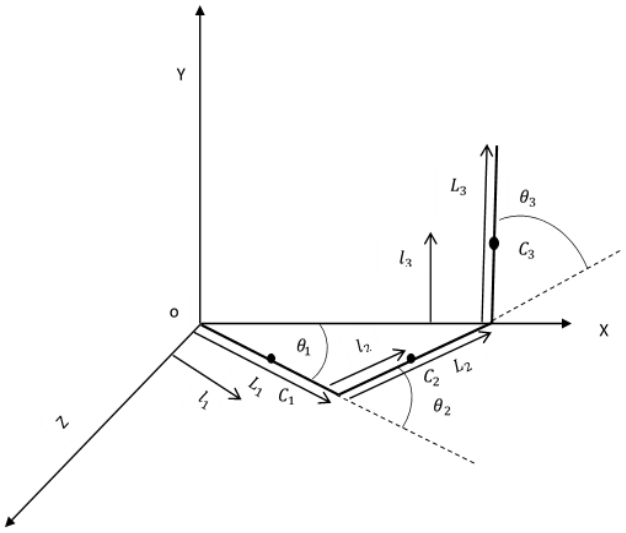

Fig 8: Thumb geometry

Link-1

Position of center of mass of first link:

$x_1 = l_1 \cos\theta_1 , y_1 = 0 , z_1 = l_1 \sin\theta_1$

linear velocity, $v_1^2 = \dot{x}_1^2 + \dot{y}_1^2 + \dot{z}_1^2$

kinetic energy, $KE_1 = \frac{1}{2} I_1 \omega_1^2 + \frac{1}{2} m_1 v_1^2$

Where, $I_1 = I$ about C_1

Angular velocity, $\omega_1^2 = \dot{\theta}_1^2$

Potential energy, $PE_1 = 0$

Link-2

Position of center of mass of second link:

$x_2 = L_1 \cos\theta_1 + l_2 \cos\theta_2 \cos\theta_1$

$y_2 = L_2 \sin\theta_2$

$z_2 = L_1 \sin\theta_1 + l_2 \cos\theta_2 \sin\theta_1$

linear velocity, $v_2^2 = \dot{x}_2^2 + \dot{y}_2^2 + \dot{z}_2^2$

kinetic energy, $KE_2 = \frac{1}{2} I_2 \omega_2^2 + \frac{1}{2} m_2 v_2^2$

Where, $I_2 = I$ about C_2

Angular velocity, $\omega_2^2 = \dot{\theta}_1^2 + \dot{\theta}_2^2$

Potential energy, $PE_2 = m_2 g(l_2 \sin\theta_2)$

Link -3

Position of center of mass of third link:

$x_3 = [L_1 + l_2 \cos\theta_2 + l_3 \cos\theta_1 \cos(\theta_2 + \theta_3)]\cos\theta_1$

$y_3 = L_2 \sin\theta_2 + l_3 \sin(\theta_2 + \theta_3)$

$z_3 = [L_1 + l_2 \cos\theta_2 + l_3 \cos(\theta_2 + \theta_3)]\sin\theta_1$

linear velocity, $v_3^2 = \dot{x}_3^2 + \dot{y}_3^2 + \dot{z}_3^2$

kinetic energy, $KE_3 = \frac{1}{2} I_3 \omega_3^2 + \frac{1}{2} m_3 v_3^2$

Where, $I_3 = I$ about C_3

Angular velocity, $\omega_3^2 = \dot{\theta}_1^2 + \left(\dot{\theta}_2 + \dot{\theta}_3\right)^2$

Potential energy, $PE_3 = m_3 g(L_2 \sin\theta_2 + l_3 \sin(\theta_2 + \theta_3))$

Lagrange-Euler equation of motion for thumb

$$\tau_1 = \frac{d}{dt}\left(\frac{\delta L}{\delta \dot{\theta}_1}\right) - \frac{\delta L}{\delta \theta_1}$$

$$= (I_1 + I_2 + I_3)\ddot{\theta}_1 + m_1 l_1^2 \ddot{\theta}_1 + m_2 (L_1 + l_2 C_2)^2 \ddot{\theta}_1$$
$$-2m_2 (L_1 + l_2 C_2) S_2 \dot{\theta}_2 \dot{\theta}_1 + m_3 \ddot{\theta}_1 (L_1 + L_2 C_2 + l_3 C_{23})^2$$
$$-2m_3 (L_1 + L_2 C_2 + l_3 C_{23})(L_2 S_2 \dot{\theta}_2 + l_3 S_{23} \dot{\theta}_{23})\dot{\theta}_1 \quad (22)$$

$$\tau_2 = \frac{d}{dt}\left(\frac{\delta L}{\delta \dot{\theta}_2}\right) - \frac{\delta L}{\delta \theta_2}$$

$$= [I_2 \ddot{\theta}_2 + m_2 l_2^2 \ddot{\theta}_2] + [I_3 \ddot{\theta}_{23} + m_3 \{L_2^2 \ddot{\theta}_2 + l_3^2 \ddot{\theta}_{23} +$$
$$L_2 l_3 C_3 (2\ddot{\theta}_2 + \ddot{\theta}_3) - L_2 l_3 S_3 \dot{\theta}_3 (2\ddot{\theta}_2 + \dot{\theta}_3) +$$
$$m_2 [\dot{\theta}_1^2 (L_1 + l_2 C_2)(l_2 S_2)]$$
$$+m_3 [\dot{\theta}_1^2 (L_1 + L_2 C_2 + l_3 C_{23})(L_2 S_2 + l_3 S_{23})]$$
$$+m_2 g l_2 C_2 + m_3 g (L_2 C_2 + l_3 C_{23}) \quad (23)$$

$$\tau_3 = \frac{d}{dt}\left(\frac{\delta L}{\delta \dot{\theta}_3}\right) - \frac{\delta L}{\delta \theta_3}$$

$$= [I_3 \ddot{\theta}_{23} + m_3 (l_3^2 \ddot{\theta}_{23} + L_2 l_3 C_3 \ddot{\theta}_2 - L_2 l_3 S_3 \dot{\theta}_3 \dot{\theta}_2)]$$
$$+m_3 [\dot{\theta}_1^2 (L_1 + L_2 C_2 + l_3 C_{23})(l_3 S_{23}) + L_2 l_3 S_3 \dot{\theta}_2 \dot{\theta}_{23}]$$
$$+m_3 g l_3 C_{23} \quad (24)$$

Development of Joint torque equation for index finger

This finger also has 3 degrees of freedom but all the joints move in the same plane and that's why its torque equations are little bit different from the thumb. The torque equation of index finger is given below:

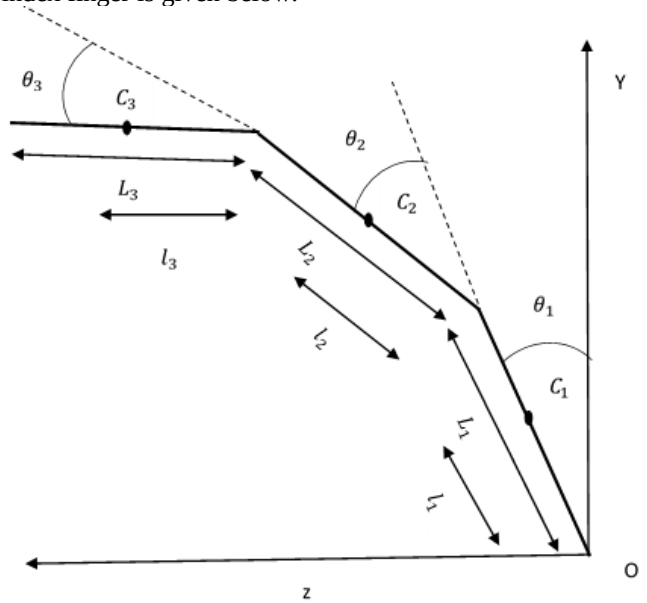

Fig 9: Index finger geometry

Link-1

Position of center of mass of first link:

$$x_1 = 0$$
$$y_1 = l_1 \cos\theta_1$$
$$z_1 = l_1 \sin\theta_1$$

linear velocity, $v_1^2 = \dot{x}_1^2 + \dot{y}_1^2 + \dot{z}_1^2$

kinetic energy, $KE_1 = \frac{1}{2} I_1 \omega_1^2 + \frac{1}{2} m_1 v_1^2$

Where, $I_1 = I$ about C_1

Angular velocity, $\omega_1^2 = \dot{\theta}_1^2$

Potential energy, $PE_1 = m_1 g (l_1 \cos\theta_1)$

Link-2

Position of center of mass of second link:

$$x_2 = 0$$
$$y_2 = L_1 \cos\theta_1 + l_2 \cos(\theta_1 + \theta_2)$$
$$z_2 = L_1 \sin\theta_1 + l_2 \sin(\theta_1 + \theta_2)$$

linear velocity, $v_2^2 = \dot{x}_2^2 + \dot{y}_2^2 + \dot{z}_2^2$

kinetic energy, $KE_2 = \frac{1}{2} I_2 \omega_2^2 + \frac{1}{2} m_2 v_2^2$

Where, $I_2 = I$ about C_2

Angular velocity, $\omega_2^2 = \left(\dot{\theta}_1 + \dot{\theta}_2\right)^2$

Potential energy, $PE_2 = m_2 g[L_1 \cos\theta_1 + l_2 \cos(\theta_1 + \theta_2)]$

Link -3

Position of center of mass of third link:

$$x_3 = 0$$
$$y_3 = L_1 \cos\theta_1 + L_2 \cos(\theta_1 + \theta_2) + l_3 \cos(\theta_1 + \theta_2 + \theta_3)$$
$$z_3 = L_1 \sin\theta_1 + L_2 \sin(\theta_1 + \theta_2) + l_3 \sin(\theta_1 + \theta_2 + \theta_3)$$

linear velocity, $v_3^2 = \dot{x}_3^2 + \dot{y}_3^2 + \dot{z}_3^2$

kinetic energy, $KE_3 = \frac{1}{2} I_3 \omega_3^2 + \frac{1}{2} m_3 v_3^2$

Where, $I_3 = I$ about C_3

Angular velocity, $\omega_3^2 = \left(\dot{\theta}_1 + \dot{\theta}_2 + \dot{\theta}_3\right)^2$

Potential energy, $PE_3 = m_3 g[L_1 \cos\theta_1 + L_2 \cos(\theta_1 + \theta_2) + l_3 \cos(\theta_1 + \theta_2 + \theta_3)]$

Lagrange-Euler equation

$$\tau_1 = \frac{d}{dt}\left(\frac{\delta L}{\delta \dot{\theta}_1}\right) - \frac{\delta L}{\delta \theta_1}$$
$$= [I_1\ddot{\theta}_1 + m_1 l_1^2 \ddot{\theta}_1]$$
$$+[I_2\ddot{\theta}_{12} + m_2\{L_1^2\ddot{\theta}_1 + l_2^2\ddot{\theta}_{12} + L_1 l_2 C_2(2\ddot{\theta}_1 + \ddot{\theta}_2)$$
$$-L_1 l_2 S_2\dot{\theta}_2(2\dot{\theta}_1 + \dot{\theta}_2)\}]$$
$$+[I_3\ddot{\theta}_{123} + m_3\{L_1^2\ddot{\theta}_1 + L_2^2\ddot{\theta}_{12} + l_3^2\ddot{\theta}_{123} +$$
$$L_1 L_2 C_2(2\ddot{\theta}_1 + \ddot{\theta}_2) - L_1 L_2 S_2\dot{\theta}_2(2\dot{\theta}_1 + \dot{\theta}_2)$$
$$+L_2 l_3 C_3(2\ddot{\theta}_1 + 2\ddot{\theta}_2 + \ddot{\theta}_3) -$$
$$L_2 l_3 S_3\dot{\theta}_3(2\dot{\theta}_1 + 2\dot{\theta}_2 + \dot{\theta}_3) + L_2 l_3 C_{23}(2\ddot{\theta}_1 + \ddot{\theta}_2 + \ddot{\theta}_3)$$
$$-L_2 l_3 S_{23}\dot{\theta}_{23}(2\dot{\theta}_1 + \dot{\theta}_2 + \dot{\theta}_3)\}]$$
$$-g[m_1 l_1 S_1 + m_2 L_1 S_1 + m_2 l_2 S_{12} + m_3 L_1 S_1$$
$$+m_3 L_2 S_{12} + m_3 l_3 S_{123}]$$
(25)

$$\tau_2 = \frac{d}{dt}\left(\frac{\delta L}{\delta \dot{\theta}_2}\right) - \frac{\delta L}{\delta \theta_2}$$
$$= [I_2\ddot{\theta}_{12} + m_2\{l_2^2\ddot{\theta}_{12} + L_1 l_2\ddot{\theta}_1 C_2 - L_1 l_2\dot{\theta}_1\dot{\theta}_2 S_2]$$
$$+[I_3\ddot{\theta}_{123} + m_3\{L_2^2\ddot{\theta}_{12} + l_3^2\ddot{\theta}_{123} + L_1 L_2 C_2\ddot{\theta}_1 - L_1 L_2 S_2\dot{\theta}_2\dot{\theta}_1$$
$$+L_2 l_3 C_3(2\ddot{\theta}_2 + 2\ddot{\theta}_2 + \ddot{\theta}_3) - L_2 l_3 S_3\dot{\theta}_3(2\dot{\theta}_2 + 2\dot{\theta}_2 + \dot{\theta}_3)$$
$$+L_1 l_3 C_{23}\ddot{\theta}_1 - L_1 l_3 S_{23}\dot{\theta}_{23}\dot{\theta}_1\}]$$
$$+[m_2 L_1 l_2\dot{\theta}_1\dot{\theta}_{12} S_2 + m_3 L_1 L_2 S_2\dot{\theta}_1\dot{\theta}_{12} + m_3 L_1 l_3 S_{23}\dot{\theta}_1\dot{\theta}_{123}]$$
$$-g[m_2 l_2 S_{12} + m_3 L_2 S_{12} + m_3 l_3 S_{123}]$$
(26)

$$\tau_3 = \frac{d}{dt}\left(\frac{\delta L}{\delta \dot{\theta}_3}\right) - \frac{\delta L}{\delta \theta_3}$$
$$= [I_3\ddot{\theta}_{123} + m_3(l_3^2\ddot{\theta}_{123} + L_2 l_3 C_3\ddot{\theta}_{12}$$
$$-L_2 l_3 S_3\dot{\theta}_3\dot{\theta}_{12} + L_1 l_3 C_{23}\ddot{\theta}_1$$
$$-L_1 l_3 S_{23}\dot{\theta}_{23}\dot{\theta}_1)] + m_3[L_2 l_3 S_3\dot{\theta}_{12}\dot{\theta}_{123} + L_1 l_3 S_{23}\dot{\theta}_1\dot{\theta}_{123}]$$
$$+m_3 g l_3 S_{123}$$
(27)

B. Static force

It is basically the torque required by a joint under static condition. A static force is applied at the end effector whose orientation is specified in accordance with the end effector frame. Due to this force the joint generates a sustainable torque which has to be solved in this section. Gravity term was completely neglected in this particular analysis. The joint has to be considered as a fixed joint in order to carry out the analysis. The joint torque is given by

$$\tau = J^T F \quad (28)$$

The above equation basically represents the relationship between joint torque vector (τ) and end effector load (F) vector [11].
Where,

J^T = transpose of Jacobin matrix of the end effector position
F= force vector

Static force analysis for thumb

Where, Jacobian matrix

$$J = \begin{bmatrix} \frac{\delta p_x}{\delta\theta_1} & \frac{\delta p_x}{\delta\theta_2} & \frac{\delta p_x}{\delta\theta_3} \\ \frac{\delta p_y}{\delta\theta_1} & \frac{\delta p_y}{\delta\theta_2} & \frac{\delta p_y}{\delta\theta_3} \\ \frac{\delta p_z}{\delta\theta_1} & \frac{\delta p_z}{\delta\theta_2} & \frac{\delta p_z}{\delta\theta_3} \end{bmatrix}$$

And force-moment matrix

$$F = \begin{bmatrix} 0 \\ 0 \\ 1 \end{bmatrix}$$

Hence, $\tau = \begin{bmatrix} 0 \\ -\{L_3\cos(\theta_2+\theta_3) + L_2\cos\theta_2\} \\ -\{L_3\cos(\theta_2+\theta_3)\} \end{bmatrix}$

$$\tau_{s1} = 0 \quad (29)$$
$$\tau_{s2} = -\{L_3\cos(\theta_2+\theta_3) + L_2\cos\theta_2\} \quad (30)$$
$$\tau_{s3} = -\{L_3\cos(\theta_2+\theta_3)\} \quad (31)$$

Static force analysis for index finger:

Where, Jacobian matrix

$$J = \begin{bmatrix} \frac{\delta p_x}{\delta\theta_1} & \frac{\delta p_x}{\delta\theta_2} & \frac{\delta p_x}{\delta\theta_3} \\ \frac{\delta p_y}{\delta\theta_1} & \frac{\delta p_y}{\delta\theta_2} & \frac{\delta p_y}{\delta\theta_3} \\ \frac{\delta p_z}{\delta\theta_1} & \frac{\delta p_z}{\delta\theta_2} & \frac{\delta p_z}{\delta\theta_3} \end{bmatrix}$$

And force-moment matrix

$$F = \begin{bmatrix} 0 \\ 1 \\ 0 \end{bmatrix}$$

Hence,

$$\tau = \begin{bmatrix} L_2\cos(\theta_1+\theta_2) + L_1\cos\theta_1 + L_3\cos(\theta_1+\theta_2+\theta_3) \\ L_2\cos(\theta_1+\theta_2) + L_3\cos(\theta_1+\theta_2+\theta_3) \\ L_3\cos(\theta_1+\theta_2+\theta_3) \end{bmatrix}$$

$$\tau_{s1} = L_2\cos(\theta_1+\theta_2) + L_1\cos\theta_1 + L_3\cos(\theta_1+\theta_2+\theta_3) \quad (32)$$
$$\tau_{s2} = L_2\cos(\theta_1+\theta_2) + L_3\cos(\theta_1+\theta_2+\theta_3) \quad (33)$$
$$\tau_{s3} = L_3\cos(\theta_1+\theta_2+\theta_3) \quad (34)$$

C. Motion dynamics with static force

It is the combination of motion dynamics with no load condition and static force analysis. It involves finding out the torque when the body carries a load as well as generate the desired motion (similar to pick and place operation). The equation of joint torque is therefore

$$\tau_{fi} = \tau_i + \tau_{si} \quad (35)$$

V. CONTROL

Control of the manipulator is one of the important areas for precise design. It is used to regulate the movement of the manipulator minutely. To serve this purpose, this article implements a PID control technique. There are various techniques of PID control, but this paper follows the ADAMS-MATLAB COSIMULATION technique to serve this purpose. Here, the movement of the model, under the effect of the control system can be easily seen in the simulation.

To run this co-simulation, the basic block has been developed in Simulink and the control plant was imported from the ADAMS software. The imported plant is called ADAMS SUB-SYSTEM [15] which has been shown in Fig 10. ADAMS SUB-SYSTEM consist of the joint torques as input variables and angular displacements of the joints as output variables. The Simulink block diagram has been shown in Fig 11. where the PID control block was used to control the manipulator. Here, the control of the thumb has been shown. The control of rest of the fingers can be carried out along similar lines.

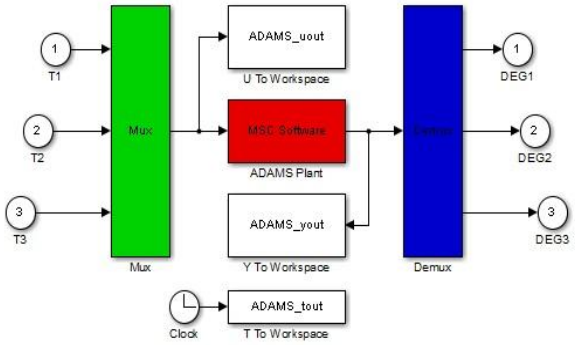

Fig 10: ADAMS Subsystem

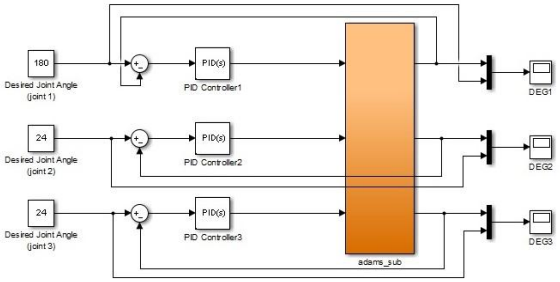

Fig 11: Simulink Block Diagram for PID Control of the thumb

VI. RESULTS AND DISCUSSIONS

In this section, the results obtained from the theoretical calculations have been verified with the results of the simulation. The time history of the position, velocity, and acceleration of the end effectors of the fingers as well as the joint torques has been plotted in MATLAB and they were compared with the results obtained from ADAMS.

A. Results from kinematic analysis

Results of the thumb

Forward kinematics of thumb

The comparison of the end effector's position, velocity and acceleration as well as the joint velocities and accelerations of the thumb are shown below:

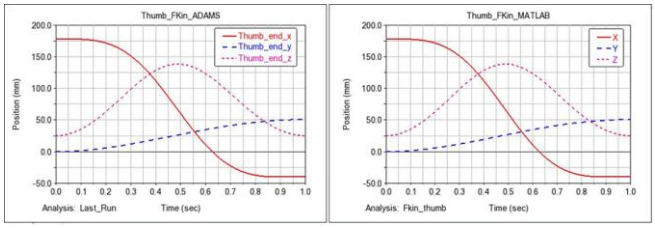

Fig 12: Comparison of position plots of end effector from ADAMS and MATLAB

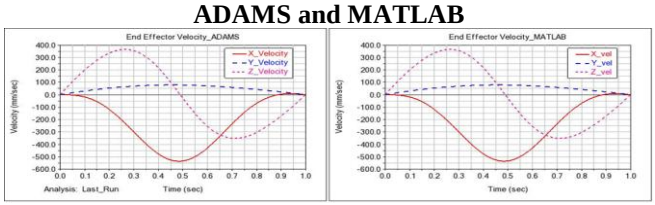

Fig 13: Comparison of velocity plots of end effector from ADAMS and MATLAB

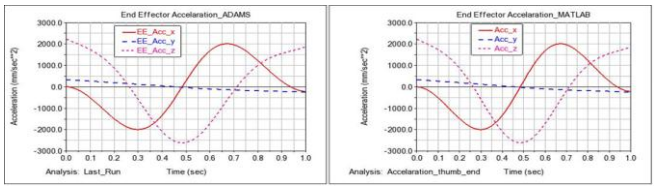

Fig 14: Comparison of acceleration plots of end effector from ADAMS and MATLAB

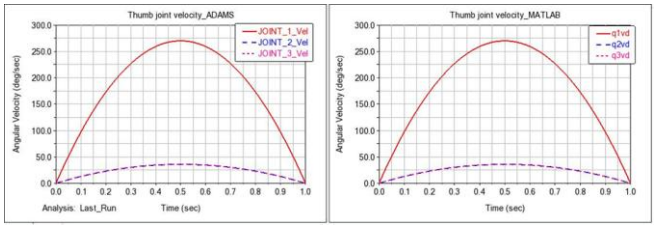

Fig 15: Comparison of joint velocities of the thumb from ADAMS and MATLAB

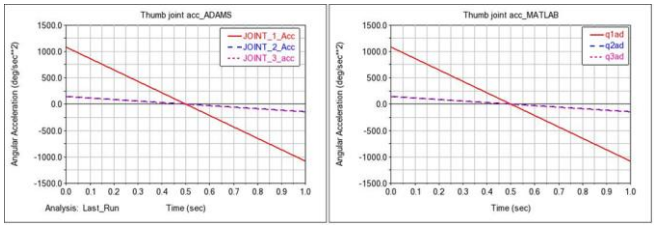

Fig 16: Comparison of joint accelerations of the thumb from ADAMS and MATLAB

Inverse kinematics of thumb

In order to validate the inverse kinematic analysis, the transformation matrix (w.r.t. the first joint frame), that was obtained from the forward kinematics was used to figure out the angles and those were counter verified with the original joint trajectories. The comparison is shown below:

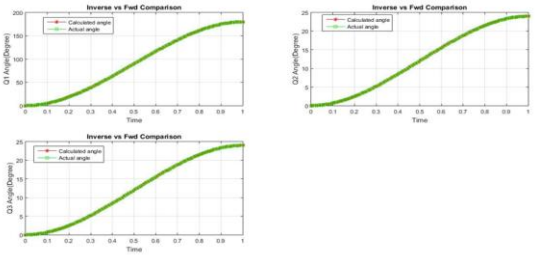

Fig 17: Verification of inverse kinematic analysis in MATLAB

Results of the Index finger

Operations similar to the thumb was carried out in this case also and the results are shown below:

Forward kinematics of index finger

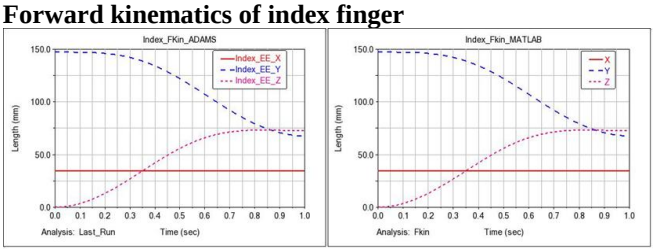

Fig 18: Comparison of position plots of end effector from ADAMS and MATLAB

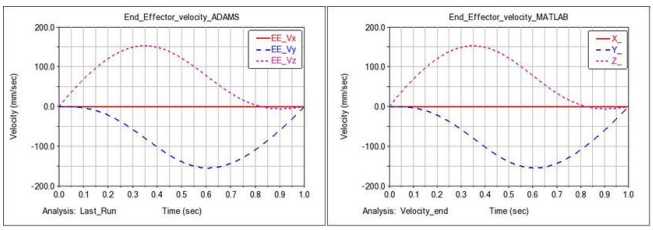

Fig 19: Comparison of velocity plots of end effector from ADAMS and MATLAB

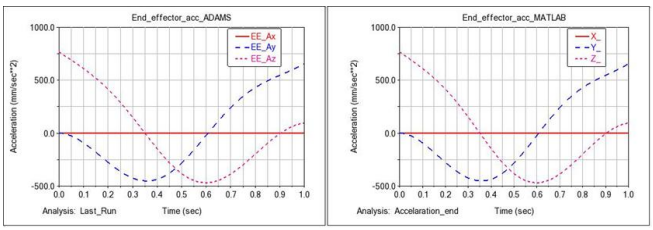

Fig 20: Comparison of acceleration plots of end effector from ADAMS and MATLAB

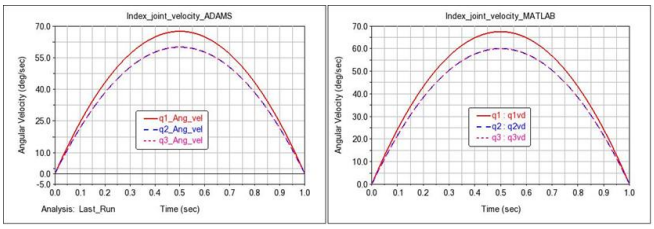

Fig 21: Comparison of joint velocities of the thumb from ADAMS and MATLAB

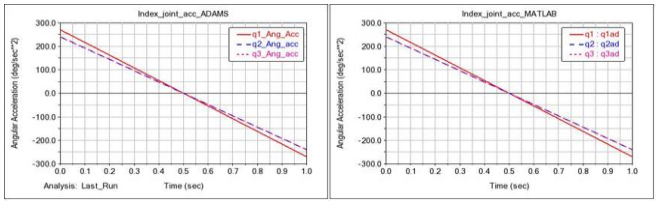

Fig 22: Comparison of joint accelerations of the thumb from ADAMS and MATLAB

Inverse kinematics of index finger

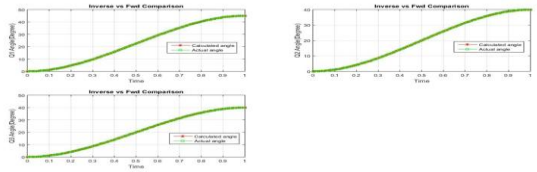

Fig 23: Verification of inverse kinematic analysis in MATLAB

The analyses of the rest of the three fingers are same as that of the index fingers with the link lengths being the only variants

B. Results from dynamic analysis

The results of the dynamic analyses have been divided into two parts viz. only due to a desired motion and secondly, considering a static force acting on the end effector along with the desired motion. It is to be noted that the latter is of greater practical importance as the static force symbolizes loads that would act on the fingers. Once again, the theoretical results have been verified with the simulation results. The results are shown below:

Results of the Thumb

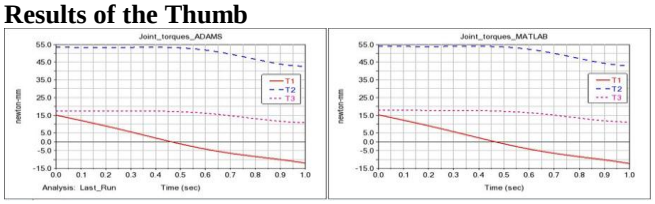

Fig 24: Comparison of joint torques of the thumb (only due to motion) from ADAMS and MATLAB

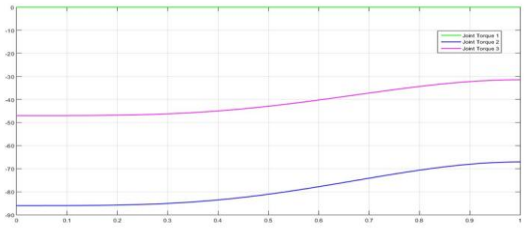

Fig 25: Joint torques only due to static force

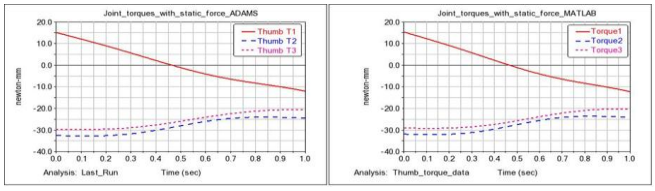

Fig 26: Comparison of joint torques of the thumb (with added static force) from ADAMS and MATLAB

Results of the Index finger

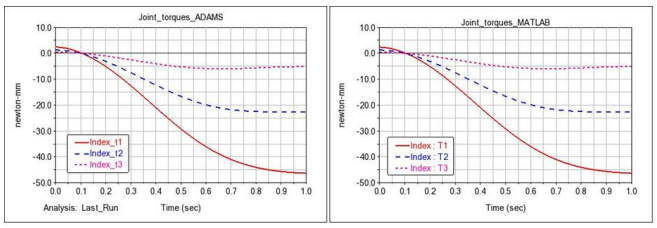

Fig 27: Comparison of joint torques of the index finger (only due to motion) from ADAMS and MATLAB

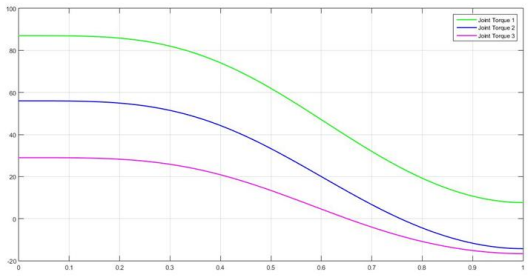

Fig 28: Joint torques only due to static force

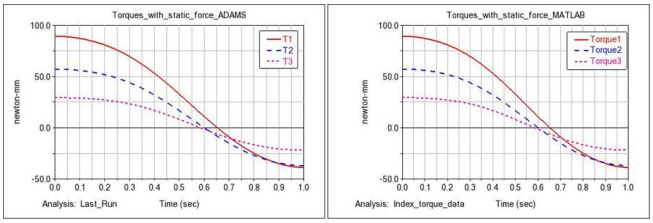

Fig 29: Comparison of joint torques of the index finger (with added static force) from ADAMS and MATLAB

C. Results of control

The PID blocks were tuned so as to get the desired response. After going through an iterative process, the block parameters were found so as to get the desired response. The block parameters are:

Table 7. Block parameters of the control system

Joint/ PID controller	P	I	D	N
1	-0.05	-0.005	0.4	100
2	0.05	-0.0588	0.0087	5
3	0.01	-0.0128	0.007	4.5

The responses (in this case, joint angles) for the 3 joints of the thumb are shown below:

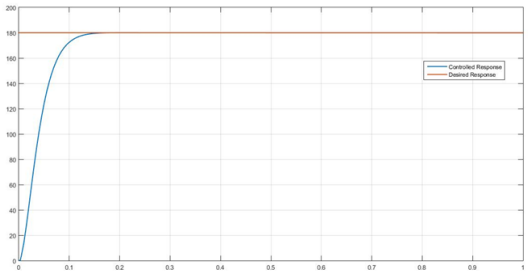

Fig 30: Response of Joint 1

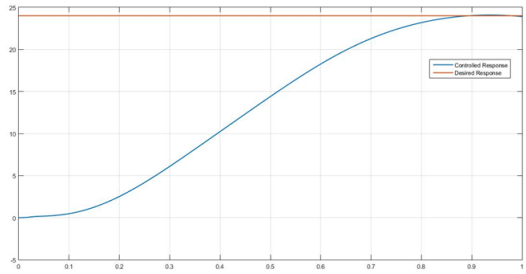

Fig 31: Response of Joint 2

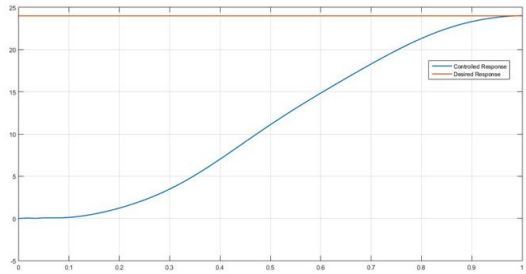

Fig 32: Response of Joint 3

The rise time or transient time for 2nd and 3rd joint is greater than that of the 1st joint.

VII. CONCLUSIONS

In this paper, a robotic hand was modelled and simulated using virtual prototyping technology. The 3-d model was developed using CAD software and imported to ADAMS for the simulation purpose. The mathematical analyses were carried out in MATLAB and the results were verified with those of the simulation [14]. A co-simulation-based control strategy was developed in order to impart smooth movement to the hand. The results obtained from theoretical calculations were consistent with those of the simulation, hence, validation the proposed methodology. The advantage of this kind of VP technology is that, a huge amount of data can be collected in a very short period of time. Therefore, a large number of hit and trials can be conducted before the development of physical prototype hence, reducing material wastage and tediousness of the process. Moreover, the material, sensor and actuator selection become easier based on the obtained results. As for further scope is concerned, all these mathematical analyses will be of immense help in developing the under actuated model of the hand.

REFERENCES

1. Khin Moe, Myint, Zaw Min Min Htun, Hla Myo Tun, “Position Control Method for Pick and Place Robot Arm for Object Sorting System.” international journal of scientific & technology research, 5 (2016) 57-61.
2. Joseph R. Davidson, Changki Mo, “mechanical design and initial performance testing of an apple picking end-effector.” ASME International Mechanical Engineering Congress and Exposition, Houston, Texas, USA, (2015) 1-9.
3. Pratik Baid, Manoj Kumar.V, “A RRP Configuration Robot Arm for Drawing Application.” Journal of Chemical and Pharmaceutical Sciences, 9 (2016) 2519-2523.

4. Pilwon Heo, Gwang Min Gu, Soo-jin Lee, Kyehan Rhee and Jung Kim, "Current Hand Exoskeleton Technologies for Rehabilitation and Assistive Engineering." international journal of precision engineering and manufacturing, 13 (2012) 807-824.
5. Pramod Kumar Parida, "Kinematic Analysis of Multi-Fingered, Anthropomorphic Robotic Hands." Doctor of Philosophy thesis, National Institute of Technology Rourkela, INDIA, (2013).
6. Kiran Y. jadhav, Sangeetha Prasanna Ram, "Biomechanical Analysis of Human Upper Limb." international journal of advanced research in electrical, electronics and instrumentation engineering, 6 (2017) 91-99.
7. Zhi-Hong Mao, Member, Heung-No Lee and Robert J. Sclabassi, and Mingui Sun, "Information Capacity of the Thumb and the Index Finger in Communication." IEEE transactions on biomedical engineering, 56 (2009) 1535-1545.
8. S.Parasuraman, Kee Chew Yee, "Bio-mechanical analysis of human hand," international conference on computer and automation engineering, Bangkok, Thailand, (2009) 93-97.
9. Md Akhlaquor Rahmana, Adel Al-Jumailya, "Design and development of a hand exoskeleton for rehabilitation following stroke." Procedia Engineering, 41 (2012) 1028 – 1034.
10. D.K.Pratihar, "Fundamentals of robotics." 2nd edition, Narosa publishing House, 2017.
11. Abhijit Mahapatra, "Multi-body dynamics modeling and simulation of six-legged robots maneuvering over varying Terrains." Doctor of Philosophy, National Institute of Technology Durgapur, INDIA, (2017)
12. John J. Craig, "Introduction to robotics mechanics and Control." 2nd edition, Pearson Education, 2004.
13. Tejaswin Parthasarathy, Vignesh Srinivasaragavan and Soundarapandian Santhanakrishnan, "ADAMS-MATLAB Co-Simulation of a Serial Manipulator." 3rd International Conference on Mechatronics and Mechanical Engineering Shanghai, China, (2016) 1-6.
14. Luo Haitao, Liu Yuwang, Chen Zhengcang and Leng Yuquan, "Co-Simulation Control of Robot Arm Dynamics in ADAMS and MATLAB." Research Journal of Applied Sciences, Engineering and Technology, 6 (2013) 3778-3783.
15. Adams team at MSC Software, "Adams Tutorial Kit for Mechanical Engineering Courses." 3rd edition, MSC Software.

AUTHORS PROFILE

Ranashree Das obtained his B-tech in Mechanical engineering from Jalpaiguri Govt. Engineering College, 2011 and M.E. from Jadavpur University, 2014. Presently, a research scholar at NIT Durgapur, Mechanical Engineering department. His research areas include: Robotics and Automation, Soft computing and Non- traditional optimization.

Dhrubajyoti Gupta is presently pursuing his B-tech in Mechanical Engineering at NIT Durgapur. His area of expertise and research interests include: Robotics and Automation, Artificial Intelligence, Control theory, Computer vision and Advanced data analytics.